

# Author Queries

*JOB NUMBER:* MS 404677

*JOURNAL:* GCMB

- Q1** Please supply article titles for the references de la Isla et al. (2003) and Horta et al. (2003). 
- Q2** Please provide a description for the part labels (a)–(e) in Figure 3. 

## Modal behaviour of bones during fracture

Jaime Horta-Rangel<sup>a</sup>, Ana L. Rodríguez<sup>a</sup> and Victor M. Castano<sup>b\*</sup>

<sup>a</sup>Universidad Autónoma de Querétaro, Cerro de las Campanas, Querétaro, Querétaro 76010, México; <sup>b</sup>Centro de Física Aplicada y Tecnología Avanzada, Universidad Nacional Autónoma de México, A.P. 1-1010, Santiago de Querétaro, Querétaro 76000, México

(Received 17 February 2009; final version received 15 May 2009)

A common cause of human disability is related to the fracture of bones, complex structural materials whose properties vary with time. An analytical study (using ANSYS, a commercial finite element package) of bones under fracture conditions is presented, focusing on the frequencies variation versus depth crack, as well as on the evolution of strength in the fracture area.

**Keywords:** femur; modal behaviour; biomechanics

### 1. Introduction

The bone structure consists of three types: compact bone, trabecular bone and marrow. Figure 1 shows schematic cuts of a long bone, which has a variable thickness, with a minimum in their extremes (epiphysis) and a maximum on the middle of the bone (diaphysis). As far as its composition is concerned, the bone is formed by two parts, one organic and the other inorganic, the first one is constituted essentially by collagen fibres whereas the second part by calcium compounds, mainly hydroxyapatite. The synergetic association of the hydroxyapatite with collagen fibres is responsible for the hardness and strength characteristics of the bone tissue (Carter 1987).

The mechanical behaviour of bone depends on many variables; the bone *in situ* is under a temperature of 37°C and with high humidity content (Solares et al. 1974; García and Doblar 1999). Of particular interest is the healing properties of bones, after being subjected to mechanical stresses (Solares et al. 1974; Kreeger 1979; Regirer and Shtein 1985; Cook et al. 1989; Morton 1991; Jacobs 1994; Rodríguez et al. 1996; García and Doblar 1999; de la Isla et al. 2003).

Accordingly, we present here a theoretical study, by using finite element Method, of the mechanical behaviour of bones at fracture conditions, aiming to contribute to the understanding of these fascinating and complex natural materials.

### 2. Theoretical background

For our present purpose, the structure of a bone is that of a composite material with two essential phases: a solid one constituted by fibres of collagen and hydroxyapatite, and

a soft phase composed by channels and interstices occupied by marrow, blood and other nutrients with products generated by the own bone. When observing the structure of the compact bone in cross-section, we observe a matrix of round agglomerates of collagen fibres (Regirer and Shtein 1985) known as Havers systems (Figure 2(a)).

For this model, the elements of the stiffness matrix, according to the elastic approach, as proposed by Kreeger (Figure 2(b)) and adjusting them to maintain their helical distribution, is:

$$[S]_{ijk} = \iiint [\mathbf{B}][\mathbf{D}][\mathbf{B}]dV = \sum_{n=1}^N S_{ijk}^{(n)} C_i C_j C_k \frac{A(n)}{V} dL(n), \quad (1)$$

where  $[\mathbf{B}]$  is the matrix of derivatives of the form functions (Cook et al. 1989);  $[\mathbf{D}]$ , matrix of elastic constant;  $N$ , number of trajectories of the thin sheets of collagen fibres;  $A(n)$ , area of the cross-section of the thin sheet;  $C$ , cosines associated with the orientation of the fibre;  $L(n)$ , fibre length; and  $V$ , volume of the bundle of fibres.

Other authors propose percolation models based on a two-phase composite (Rodríguez et al. 1996). The constitutive relationship of this model is given by the equation:

$$\frac{G_C}{G_R} = \frac{(1 - \Phi^2 - \Phi v_S)G_S + \Phi v G_R}{(1 - \Phi - v_S)G_S + v_S G_S}. \quad (2)$$

Such that,  $G_C$ ,  $G_R$ , and  $G_S$  correspond to the elastic modulus of the composite, of the rigid phase and of the soft phase, respectively.  $\phi$  describes the percolation threshold

\*Corresponding author. Email: castano@fata.unam.mx

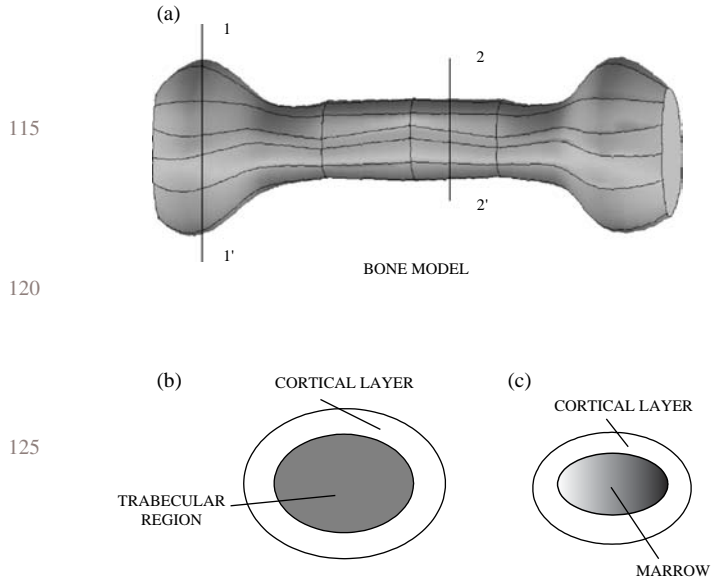


Figure 1. Structure of a long bone. (a) Front view, (b) cross-section on the epiphysis and (c) cross-section of the diaphysis.

defined by the expression:

$$\Phi = \begin{cases} 0 & \dots \forall v_C < v_R \\ v_R \left( \frac{v_R - v_C}{1 - v_C} \right)^\beta & \dots \forall v_C \geq v_R. \end{cases} \quad (3)$$

Here,  $v_R$  and  $v_S$  are the volume fractions of the rigid phase and soft phase, respectively. This percolation model is based on the diagram of Figure 3. The fibres are random distributed (Figure 3(c)) and under certain rules the percolation matrix of Figure 3(a), which is representative of the volume as well as of the location of the two phases, can be constructed. In the case of a bone, the fibres distribution is not so random but rather presents a marked orientation along an axis, as in the case of the long bones; in another type of bones, like for example in the flat ones, this distribution is more random, due to the complex surfaces.

An approach for the more complicated situation shown in Figure 3(d), (e) is by noticing that this last model bears a great resemblance to the porosity models where the density  $\rho$  of the material can be used as a description of the average behaviour of the system. According to the continuum mechanics, the local equation conservation of the mass (Morton 1991) can be expressed by:

$$\dot{\rho} + \rho \operatorname{div} \underline{v} = 0; \quad \rho' + \operatorname{div}(\rho \underline{v}) = 0, \quad (4)$$

where  $\dot{\rho}$  is the time derivative of density spatial field;  $\rho'$ , spatial derivative of density field; and  $\underline{v}$ , velocity field.

When considering the matrix structure of Figure 3(d) and by modifying the concept of soft phase to account for the holes phase or pores occupied by a material of low density (marrow), the parameter  $n$  of the volume

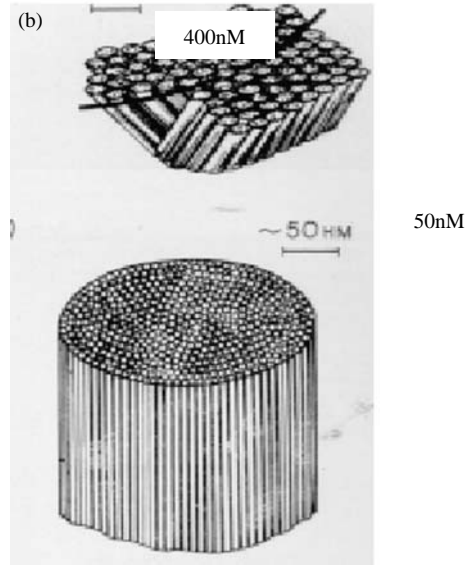
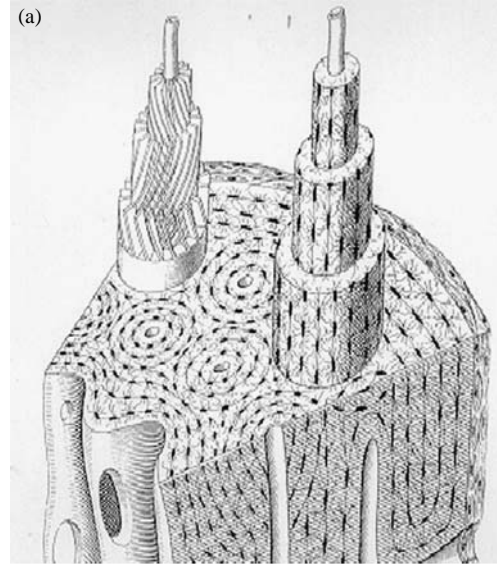


Figure 2. Microscopic structures of the compact bone. (a) Havers systems and (b) fibres model proposed by Kreeger.

relationship of voids (or pores)  $V_P$  is related to the total volume of the bone  $V_T$  as:

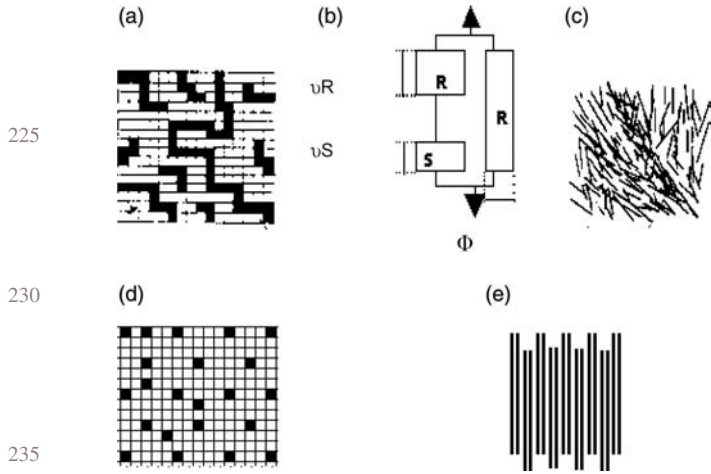
$$n = \frac{V_P}{V_T}. \quad (5)$$

This relationship, as function of the density, is expressed as:

$$n = 1 - \frac{\rho}{\rho_0} \quad (6)$$

where  $\rho_0$  is the reference density (bone without pores). In terms of the Jacoby matrix  $[\mathbf{J}]$ , it is written as (6)

$$n = 1 - \frac{1}{\det[\mathbf{J}]}, \quad (7)$$



Q2 Figure 3. Percolation models.

where  $[J]$  is the tensor matrix  $\nabla f$ ;  $f$ , deformation function, such that  $f: B_0 \rightarrow B$ ;  $B_0$ , configuration of undeformed of body (in this case, without pores); and  $B$ , deformed body. Substituting (7) in (4), we obtain:

$$\frac{\partial \rho}{\partial t} + \text{div}[(1 - n)\rho_0 \underline{v}] = 0. \quad (8)$$

This relationship is adjusted by Jacob (de la Isla et al. 2003), who proposes the following expression:

$$\frac{\partial \rho}{\partial t} = \left( \frac{\partial r}{\partial t} \right) S_v \rho_0, \quad (9)$$

where  $(\partial r / \partial t) = \underline{v}$  is the velocity of surface remodelling of the bone (growth and consolidation) and  $S_v$ , available surface per unit of bone volume.

This last parameter is also denominated specific surface and it depends on the porosity. Its value is independent of the type of bone, age and state; it is well described by a 5th degree polynomial. It is a function of the relationship of voids and a results of the bone density:  $vS_v = g(\rho)$ .

The stresses tensor  $S$  is expressed in the following form:

$$\underline{S} = 2\mu \underline{E} + \lambda (\text{tr} \underline{E}) \underline{I}. \quad (10)$$

Here, the stress  $S$  refers to that experienced by the bone during a the time necessary to make it grow. When considering (9), we obtain expressions that allow to relate the modulus of elasticity  $E$  with the density  $\rho$  and the modulus of Poisson  $\nu$  of the bone (García and Doblar 1999):

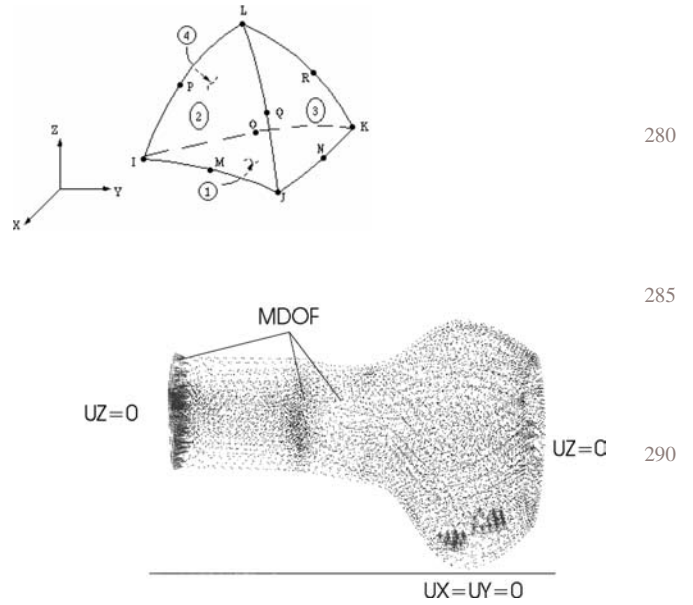


Figure 4. Boundary conditions and finite element type used.

$$E(\text{MPa}) = \begin{cases} 2014 & \forall \rho = 1.2 \text{ T/m}^3 \\ 1763 & \forall \rho = 1.2 \text{ T/m}^3 \end{cases}, \quad (11)$$

$$\nu = \begin{cases} 0.2 & \forall \rho = 1.2 \text{ T/m}^3 \\ 0.32 & \forall \rho = 1.2 \text{ T/m}^3 \end{cases}.$$

The governing equations for undamped modal analysis is (Cook et al. 1989):

$$[M]\{\ddot{U}\} + [K]\{U\} = \{0\}. \quad (12)$$

The boundary conditions, as well as the finite element applied are shown in Figure 4.

### 3. Results and discussion

The above equations allow to decide what are the proper parameters for describing a bone during fracture. For this, we use the measured density of a cow compact bone, which is  $1.95 \text{ T/m}^3$ . On the other hand, according to several authors, the density of the compact bone is of the order of 10% (García and Doblar 1999), while in the porous it is of 40–60%, meaning this that the equivalent density in our case (bone without pores)  $\rho_0$  is of  $2.166 \text{ T/m}^3$ . Next, by applying Equation (11) to determine the values of  $\rho$ , and  $\nu$  when varying  $E$ , the results obtained are shown in Tables 1 and 2. The modulus  $E$  of 15,000 Mpa was obtained experimentally by analysing non-human cortical bones.

Obviously, a fractures does not present a defined path, neither when it first appears, nor during its evolution along

Table 1. Constitutive parameters of healthy bone.

Area without fractures (measured parameters on specimens)			
Material	$E$ (Mpa)	$\nu$	$\rho$ (kg/m <sup>3</sup> )
Marrow	–	0.45	900
Compact bone	15,000	0.32	1952
Porous bone	3177	0.32	1200

Table 2. Constitutive parameters of the bone in the fracture area.

Area of fractures			
Material	$E$ (MPa)	$\nu$	$\rho$ (kg/m <sup>3</sup> )
Marrow	–	0.45	900
Compact bone (obtained values according to Equation (11))	15,000	0.32	1952
	10,000	0.32	1720
	5000	0.32	1385
	1000	0.20	837

the cross-section. Because of this we chose an irregular section in the central part of the bone, with an average thickness of 2.0 cm, taking into that account, if half of the bone is analysed, then the total average thickness of the consolidation zone will be 4 cm. We continue to vary their properties according to the values of Table 2. For the zone without fracture the values of Table 1 are still valid. The results are shown in Figure 5.

The application of a sudden load is in general the main cause of fractures and severe damages in bones, especially if the applied forces are arbitrary and present in any possible direction. Figure 6 shows the von-Misses diagram for  $P = 1000$  kg and, as observed there, the concentrations of stresses occurs, as expected, around the central area. In this case, the boundary conditions are the same as the ones shown in Figure 4.

These results indicate the convenience of studying the inferior central area in detail. Indeed, when the fracture is evolving, discontinuities and concentrations of stresses are

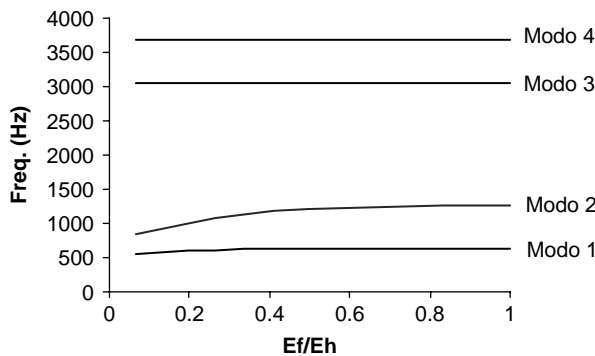


Figure 5. Variation of the resonance frequencies in the fractured bone.

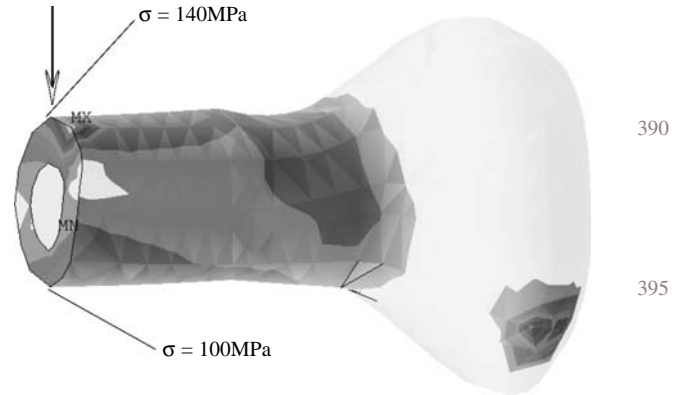


Figure 6. von-Misses stresses for  $P = 1000$  kg.

generated and various procedures exist to evaluate the  $J$  integral around the crack (Jacobs 1994; SAS IP, Inc 1996; de la Isla et al. 2003; Horta et al. 2003). Some authors propose methods to evaluate the close–open effect at the crack, although the present method, based on a proper modification of the boundary conditions, would also allow to follow the evolution of the crack, as it will described separately.

#### 4. Conclusion

The simulations emphasize the relationship porosity versus elasticity. The results show the complexity of the mechanical response of a bone near the fracture condition, indicating that the structure allows to maintain various of the fundamental frequencies of the bone, at different stress conditions. The full understanding of this phenomena, in addition to help to model the behaviour of bones, would allow the design of more efficient and enduring composite materials.

#### Acknowledgements

The authors would like to acknowledge the support of Prof. Alfredo Olivares.

#### References

Carter DR. 1987. Mechanics loading history and skeletal biology. *J Biomech.* 20:1095.

Cook R, Malkus D, Plesha M. 1989. Concepts and applications of finite element analysis. New York: Wiley.

de la Isla A, Brostow W, Bujard J, Estévez M, Vargas S, Rodríguez R, Castaño VM. 2003. *Aplicaciones Res Innov.* 7:110.

García JM, Doblar M. 1999. Simulación por elementos finitos del problema de remodelación ósea interna. Aplicación a la extremidad proximal del fémur, Memorias del Congreso Internacional de Métodos Numéricos en Ingeniería, SEMNI, Spain.

Horta J, Brostow W, Martínez G, Castaño VM. 2003. *Int J Numerical and Applied Eng Technol.* 27:49.

Jacobs CR. 1994. Numerical Simulation of bones adaptation the mechanical loading [Ph.D. thesis]. [Stanford (CA)]: Stanford University.	
Kreeger AF. 1979. Evaluation of the strain properties of a composite material made on the bane of space fibers. <i>J Comp Mater.</i> 5:790.	
Morton G. 1991. <i>An introduction to continuum mechanics.</i> New York: Academic Press.	
Regirer CA, Shtein AA. 1985. <i>Modern problems in biomechanics.</i> Riga: Zinatne.	
Rodríguez R, Hernández G, Castaño VM. 1996. Percolation modeling of the mechanical behavior of the composite polybutadiene–cellulose diacetate. <i>Int J Polymer Mater.</i> 32: 111.	
SAS IP, Inc. (Swanson Analysis Systems, Incorporated). 1996. <i>Expanded ANSYS workbook for Revision 5.2, USA.</i>	500
Solares R, Villegas F, Guerrero J, Olivares A, Herrera G. 1974. <i>Biomecánica del Peroné.</i> <i>Rev Prensa Méd Mex,</i> No. 11–12, Mexico City.	505
	510
	515
	520
	525
	530
	535
	540
	545
	550